A Unified Model for Gamma-Ray Bursts

Ryo Yamazaki
Department of Earth and Space Science, Osaka University, Toyonaka 560-0043, Japan
Kunihito Ioka
Physics Department and Center for Gravitational Wave Physics, 104 Davey Laboratory, Pennsylvania State University, University Park, PA 16802, USA
Takashi Nakamura, Kenji Toma
Theoretical Astrophysics Group Department of Physics, Kyoto University Kyoto 606-8502, Japan

A possible unified model of short and long gamma-ray bursts (GRBs), X-ray rich GRBs, and X-ray flashes is proposed. It is assumed that the jet of a GRB consists of many emitting sub-shells (i.e., an inhomogeneous jet model). The multiplicity of the sub-shells along a line of sight n_s is an important parameter. If n_s is large ($\gg 1$) the event looks like a long GRB, while if $n_s = 1$, the event looks like a short GRB. Finally, when $n_s = 0$, the event looks like an X-ray flash or an X-ray rich GRB. Furthermore, our model may also explain the bimodal distributions of T_{90} duration of BATSE-GRBs. Clearly, our model predicts that short GRBs should be associated with energetic SNe.

1. INTRODUCTION

For the long gamma-ray bursts (GRBs), the cosmological distance, the collimated jet, the massive star progenitor, and the association with the supernova are almost established or strongly suggested [30, 36, 60]. However, for short GRBs, little is known since no afterglow has been observed. Observed bimodal distribution of T_{90} duration implies the origin of the short burst is different from that of long GRB, e.g., coalescencing binary neutron stars. The origin of the X-ray flashes (XRFs) also remains unclear although many models have been proposed (see [54] and references therein). The observed event rate of short GRBs and XRFs are about a third of and similar to the long GRBs, respectively [16, 22, 27]. Although there may be a possible bias effect to these statistics, in an astrophysical sense, these numbers are the same or comparable. If these three phenomena arise from essentially different origins, the similar number of events is just by chance. While if these three phenomena are related like a unified scenario for active galactic nuclei [3, 4, 47], the similar number of events is natural and the ratio of the event rate tells us something about the geometry of the central engine. We propose a unified model in which the central engine of short GRBs, long GRBs and XRFs is the same and the apparent differences come essentially from different viewing angles. This paper is a slight extention of ref [55] (see also ref [45]).

2. UNIFIED MODEL

It is suggested that short GRBs are similar to the first 1 sec of long GRBs [12]. Although short GRBs are harder than long GRBs [23], this difference is mainly due to the difference in the low-energy spectral slope while the peak energy is similar [12]. Fine temporal structures in observed light curves of short GRBs are similar to those of the first several seconds of long GRBs [33]. Other properties, such as $\langle V/V_{\max}\rangle$, the angular distribution, the energy dependence of duration and the hard-to-soft spectral evolution of short GRBs, are also similar to those of long GRBs [26]. If short GRBs also obey the peak energy-luminosity relation found for the long GRBs [57], it is suggested that short and long GRBs have a similar redshift distribution [12].

These similarities suggest that the difference between short and long GRBs is just the number of pulses, and each pulse is essentially the same [39]. As shown in Fig. 1, using 4Br catalogue of BATSE [35], the fluence is roughly in proportion to the duration in the range of 0.01 to 1000 sec [5]. Thus, we may consider that each pulse is produced by essentially the same unit or the sub-jet[1], and the GRB jet consists of many sub-jets. If many sub-jets point to our line of sight, the event looks like the long GRB while if a single sub-jet points to us, the event looks like a short GRB. Since we can observe only the angular size of $\sim \gamma^{-1}$ within the GRB jet with the Lorentz factor γ, different observers will see different number of sub-jets depending on the distribution of sub-jets within the GRB jet. Since the angular size of a causally connected region is also $\gamma^{-1} < 0.01$, the opening half-angle of a sub-jet can be much smaller than that of the whole GRB jet (~ 0.1), say ~ 0.02.

XRFs also appear to be related to GRBs. Softer and dimmer GRBs smoothly extend to the XRFs [16, 22, 27, 48], while the peak energy-isotropic luminosity/energy relations hold for GRBs as well as XRFs [2, 42, 57]. The total energy including the ra-

[1]The origin of sub-jets (or equally emitting sub-shells) is discussed in § 4.1.

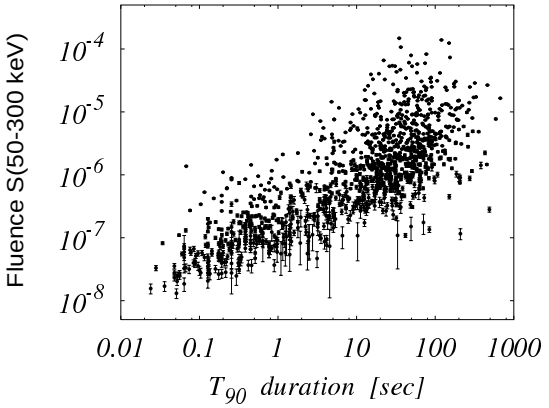

Figure 1: The fluence $S(50-300$ keV) as a function of T_{90} duration for BATSE bursts from 4Br catalog (Courtesy of Drs. S. Michikoshi and T. Suyama). From ref [55]

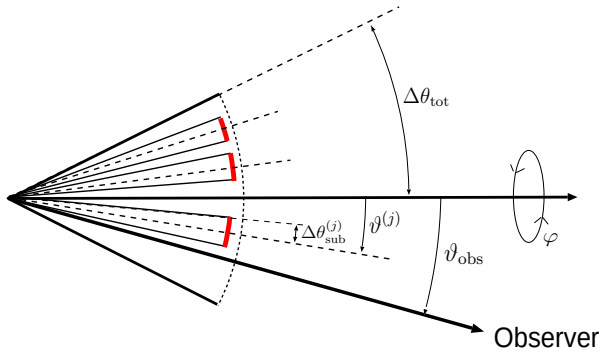

Figure 2: Schematic diagram of the multiple subjet model. Each subjet with opening half-angle $\Delta\theta_{\rm sub}$ is launched within a cone with an opening half-angle $\Delta\theta_{\rm tot}$. From ref [49].

dio afterglow of XRF 020903, which has a measured redshift, might be similar to that of GRBs [43]. Other properties, such as the duration, the temporal structure and the Band spectrum of the XRFs are also similar to those of the GRBs, suggesting that XRFs are in fact soft and dim GRBs. In the sub-jet model, XRFs are naturally expected when our line of sight is off-axis to any sub-jets [19, 31, 50, 52, 54].

3. AN EXAMPLE OF NUMERICAL SIMULATION OF OUR UNIFIED MODEL

In the following, we show a numerical simulation to demonstrate how an event looks so different depending on the viewing angle in our unified model [49, 55]. Let us consider $N_{\rm tot} = 350$ sub-jets, for simplicity, confined in the whole GRB jet whose axis is the same as a $\vartheta = 0$ axis (see fig. 2). For each sub-jet the emission model is the same as in [52]. Let the opening half-angle of the j-th sub-jet ($j = 1, \cdots, N_{\rm tot}$) be $\Delta\theta^{(j)}_{\rm sub}$, while the opening half-angle of the whole jet be $\Delta\theta_{\rm tot}$. The direction of the observer and the axis of the j-th sub-jet are specified by $(\vartheta_{\rm obs}\,, \varphi_{\rm obs})$ and $(\vartheta^{(j)}, \varphi^{(j)})$, respectively. We assume the j-th sub-jet departs at time $t^{(j)}_{\rm dep}$ from the central engine and emits at radius $r = r^{(j)}$ and time $t = t^{(j)} \equiv t^{(j)}_{\rm dep} + r^{(j)}/\beta^{(j)}c$, where t and r are measured in the central engine frame and we set $t^{(j=1)}_{\rm dep} = 0$. For simplicity, all sub-jets are assumed to have the same intrinsic properties, that is $\Delta\theta^{(j)}_{\rm sub} = 0.02$ rad, $\gamma^{(j)} = 100$, $r^{(j)} = 10^{14}$ cm, $\alpha^{(j)}_B = -1$, $\beta^{(j)}_B = -2.5$, $\gamma h\nu'^{(j)}_0 = 500$ keV and the amplitude $A^{(j)} =$ const. for all j. The departure time of each sub-jet, $t^{(j)}_{\rm dep}$ is randomly distributed between $t = 0$ and $t = t_{\rm dur}$, where $t_{\rm dur}$ is the active time of the central engine measured in its own frame and set to $t_{\rm dur} = 30$ sec. The opening half-angle of the whole jet is set to $\Delta\theta_{\rm tot} = 0.2$ rad as a typical value. We consider the case in which the angular distribution of sub-jets is given by

$$P(\vartheta^{(j)}, \varphi^{(j)})\, d\vartheta^{(j)}\, d\varphi^{(j)} \propto \exp[-(\vartheta^{(j)}/\vartheta_c)^2/2]\, d\vartheta^{(j)}\, d\varphi^{(j)}$$

for $\vartheta^{(j)} < \Delta\theta_{\rm tot} - \Delta\theta_{\rm sub}$, where we adopt $\vartheta_c = 0.1$ rad [58]. In this case, sub-jets are concentrated on the $\vartheta = 0$ axis (i.e., the multiplicity in the center $n_s \sim 10$). For our adopted parameters, sub-jets are sparsely distributed in the range $\vartheta_c \lesssim \vartheta \lesssim \Delta\theta_{\rm tot}$, however, the whole jet would be entirely filled if the sub-jets were uniformly distributed (i.e., the mean multiplicity $n_s \sim 3$). Therefore, isolated sub-jets exist near the edge of the whole jet with the multiplicity $n_s \ll 1$ and there exists a viewing angle where no sub-jets are launched. Figures 3, 4 and 5 show the angular distributions of sub-jets and the directions of four selected lines of sight, the observed time-integrated spectra, and the observed light curves in the X-ray and γ-ray bands, respectively. Note here in Figure 3, "A" represents the center of the whole jet and is hidden by the lines of sub-jets.

3.1. Long GRB

When we observe the source from the $\vartheta = 0$ axis (case "A"), we see spiky temporal structures (the upper-middle panel of Fig. 1) and $E_p \sim 300$ keV which are typical for the long GRBs. We may identify case "A" as long GRBs.

3.2. XRF and X-ray rich GRB

When the line of sight is away from any sub-jets (cases "B_1" and "B_2"), soft and dim prompt emission, i.e. XRFs or X-ray rich GRBs are observed with $E_p = 10 \sim 20$ keV and ~ 4 orders of magnitude smaller fluence than that of case "A" (Fig. 2). The burst duration is comparable to that in case "A". These are

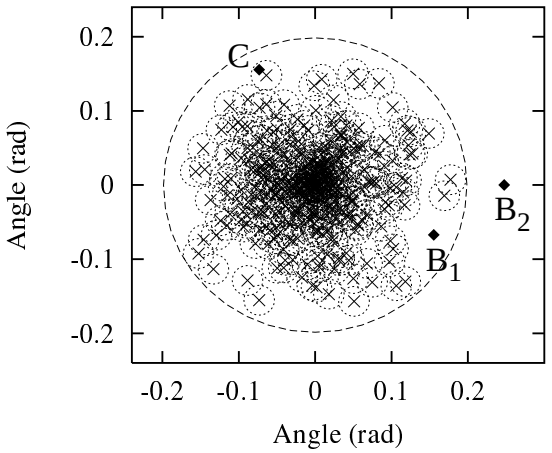

Figure 3: The angular distribution of $N_{\rm tot} = 350$ sub-jets confined in the whole GRB jet in our simulation. The whole jet has the opening half-angle of $\Delta\theta_{\rm tot} = 0.2$ rad. The sub-jets have the same intrinsic luminosity, opening half-angles $\Delta\theta_{\rm sub} = 0.02$ rad and other properties; $\gamma = 100$, $r = 10^{14}$ cm, $\alpha_B = -1$, $\beta_B = -2.5$, $h\gamma\nu' = 500\,{\rm keV}$. The axes and the angular size of sub-jets are represented by crosses and the dotted circles, respectively. "A" represents the center of the whole jet and is hidden by the lines of sub-jets. From ref [55].

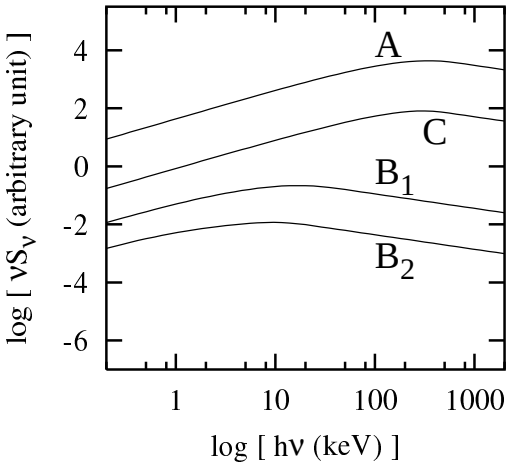

Figure 4: Time-integrated energy spectrum of the emission from the multiple sub-jets for the observers denoted by "A", "B_1", "B_2", and "C" in Figure 3. The source are located at $z = 1$. From ref [55].

quite similar to the characteristics of XRFs [19, 31, 50, 52, 54]. We may identify the cases "B_1" and "B_2" as XRFs or X-ray rich GRBs.

In our previous works [50, 52, 54], we considered the homogeneous, instantaneous emission of the whole jet. Then XRFs and X-ray rich GRBs occur only when the whole jet is viewed off-axis (corresponding case B_2). We now introduce sub-structure of the jet emission. Then, there exists the case when the observer sees all sub-jets off-axis but his line of sight is within the whole jet (case B_1). This leads two types of X-ray afterglows because in the afterglow phase, the viewing angle of the whole jet becomes important. For details see section 4.3.

3.3. Short GRB

If the line of sight is inside an isolated sub-jet (case "C"), its observed pulse duration is ~ 50 times smaller than case "A". Contributions to the observed light curve from the other sub-jets are negligible, so that the fluence is about a hundredth of the case "A". These are quite similar to the characteristics of short GRBs. However the hardness ratio ($= S(100-300\,{\rm keV})/S(50-100\,{\rm keV})$) is about 3 which is smaller than the mean hardness of short GRBs (~ 6). It is suggested that the hardness of short GRBs is due to the large low-energy photon index $\alpha_B \sim -0.58$ [12] so that if the central engine launches $\alpha_B \sim -0.58$ sub-jets to the periphery of the core where n_s is small, we may identify the case "C" as the short-hard GRBs. In other words, the hardness of 3 comes from $\alpha_B = -1$ in our simulation so that if $\alpha_B \sim -0.58$, the hardness will be 6 or so. We suggest here that not only the isotropic energy but also the photon index may depend on ϑ. Another possibility is that if short GRBs are the first 1 sec of the activity of the central engine, the spectrum in the early time might be $\alpha_B \sim -0.58$ for both the sub-jets in the core and the envelope. This is consistent with a high KS test probability for E_p and α_B [12]. These possibilities may have something to do with the origin of $\alpha_B \sim -1$ for the long GRBs.

3.4. X-ray pre-cursor/post-cursor

It is quite interesting that in Figure 5, we see the X-ray precursor at $T_{\rm obs} \sim 60$ sec in "B_2" and the postcursor at $T_{\rm obs} \sim 65$–75 sec in "B_1". These can be understood by the model proposed by [31].

4. DISCUSSIONS

4.1. Jet structures

Origin of Sub-jets. — In this paper, we do not discuss the origin of the sub-jets, but argue the implications of the multiple sub-jet model [25, 31] This model is an anologue of the patchy shell model for an afterglow [32, 34, 37]. Note that in our model, a relativistically moving emitting sub-shell is called a sub-jet. The origin of sub-jets is not yet clear. One possibility is that they may arise from relativistically outflowing blobs generated by various fluid instabilities like

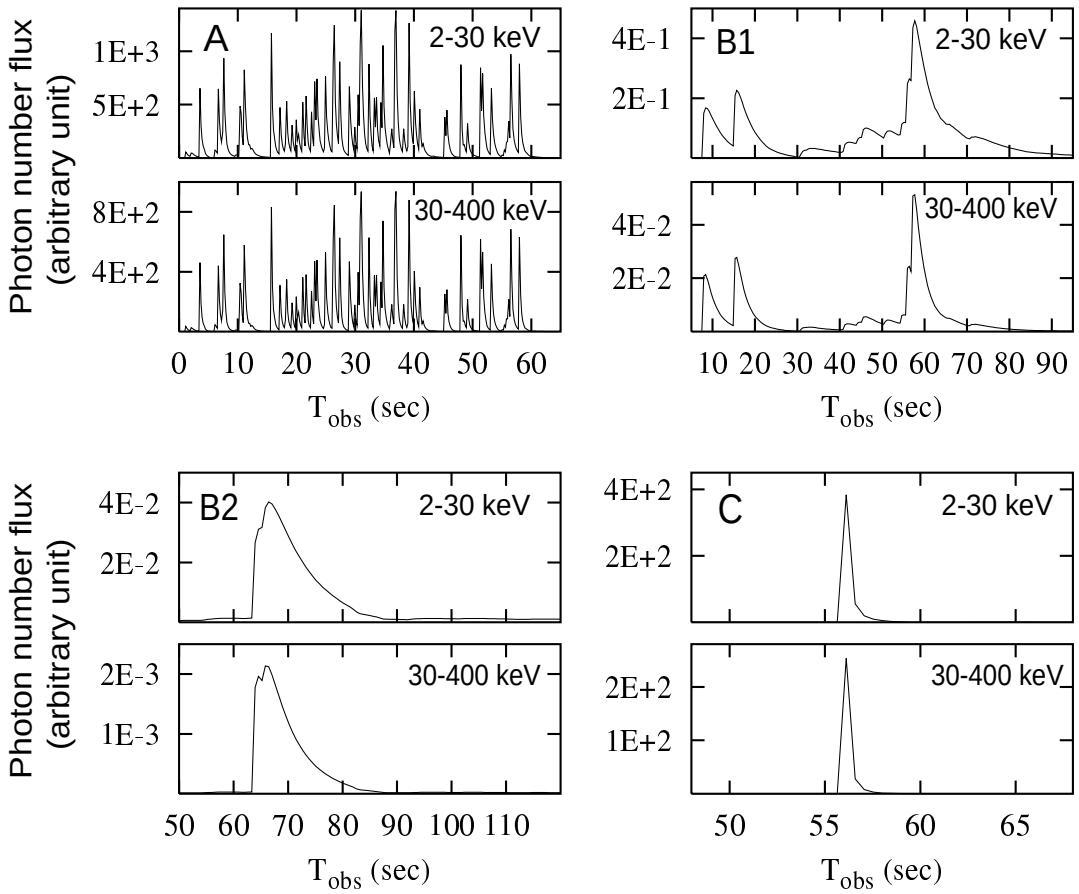

Figure 5: The observed X-ray and γ-ray light curves from the multiple sub-jets, corresponding the cases "A"(the upper left), "B_1"(the upper right), "B_2"(the lower left) and "C"(the lower right) in Figure 3. The sources are located at $z = 1$. From ref [55].

Kelvin-Helmholtz, Rayleigh-Taylor instability, and so on [1, 13, 61].

Jet structures (sub-jet configurationa) could be determined in order to reproduce all of the observed statistical properties even including those of afterglows or gravitational waves [41].

The Number of Isolated Sub-jets. — Let $\Delta\theta_{\rm sub}$, ϑ_c and $\bar{n}_s$ be the typical opening half-angle of the sub-jet, the core size of the whole jet and the mean multiplicity in the core. Then the total number of the sub-jets ($N_{\rm tot}$) is estimated as $N_{\rm tot} = \bar{n}_s(\vartheta_c/\Delta\theta_{\rm sub})^2 \sim 10^3$, so that the total energy of each sub-jet is $\sim 10^{48}$ erg. In our model, the event rate of long GRBs is in proportion to ϑ_c^2. Let M be the number of sub-jets in the envelope of the core with a multiplicity $n_s = 1$. Then the event rate of short GRBs is in proportion to $M\Delta\theta_{\rm sub}^2$, so that $M \sim 10$ is enough to explain the event rate of short GRBs.

Angular Distribution of Sub-jets. — Of course, the above numerical values are typical ones and should have a dispersion [28]. Our core-envelope sub-jet model can have a similar structure to the two component jet model [6, 18, 38, 61] by varying such as $\bar{n}_s$ and M. However the distribution of sub-jets could also have other possibilities, e.g., a hollow-cone distribution like a pulsar, a power law distribution, a Gaussian distribution [40, 58, 59] and so on.

4.2. Properties of Prompt Emission

Bimodal Distribution of T_{90} Duration. — It is also found that our model can reproduce the bimodal distribution of T_{90} duration of GRBs observed by BATSE [45]. In our model, the duration of $n_s = 1$ burst is determined by the angular spreading time of one sub-jet emission, while that of $n_s \geq 2$ burst is determined by the time interval between the observed first pulse and the last one (see also Fig. 2 of ref [45]). These two different time scales naturally lead a division of the burst T_{90} durations into the short and long ones. We show an example in Figure. 6. The dispersion of the lognormal-like distribution seems relatively small compared with the observations. This is ascribed to a simple modeling in this paper. We fix the jet configuration and use the same intrinsic properties of the subjets. If we vary $t_{\rm dur}$ for each source and $\gamma^{(j)}$ for

each subjet randomly, for example, the dispersion of lognormal-like T_{90} duration distribution will increase from the general argument that the dispersion of the lognormal distribution increases with the increase of the number of the associated random variables [20]. In more realistic modeling the observed dispersion will be reproduced.

It has commonly been said that the observed bimodal distribution of T_{90} durations of BATSE bursts shows the different origins of short and long GRBs. However, the bimodal distribution is also available as a natural consequence of our unified model of short and long GRBs.

Temporal Structures of Long GRBs and XRFs. — There are three important time scales. The first is the duration of the central engine measured by the observer $T_{\rm dur} = (1+z)\, t_{\rm dur}$. The second is the observed pulse duration of j-th sub-jet, $\delta T^{(j)}$, which is given by the angular spreading time scale of each subjet. Since emission components far from the viewing angle of γ^{-1} is dim due to the relativistic beaming effect, it can be approximated as

$$\begin{aligned}\delta T^{(j)} &\sim (1+z)\frac{r^{(j)}}{c}\Big[\cos\tilde{\theta} - \cos(\tilde{\theta}+\gamma^{-1})\Big] \\ &\sim (1+z)\frac{r^{(j)}}{2c\gamma^2}(1+2\gamma\tilde{\theta}) \quad ,\end{aligned}$$

where $\tilde{\theta} \equiv \max\{0, \theta_v^{(j)} - \Delta\theta_{\rm sub}^{(j)}\}$, and $\theta_v^{(j)}$ is the viewing angle of the j-th sub-jet given by $\cos\theta_v^{(j)} = \vec{n}_{\rm obs}\cdot\vec{n}_{\rm sub}^{(j)}$ where unit vectors $\vec{n}_{\rm obs}$ and $\vec{n}_{\rm sub}^{(j)}$ are specified by directions $(\vartheta_{\rm obs}, \varphi_{\rm obs})$ and $(\vartheta^{(j)}, \varphi^{(j)})$, respectively. The third is the time ΔT, that is the difference between times of arrival at the observer of photons that arise simultaneously at the nearest and the farthest side of the whole jet to the line of sight, i.e.,

$$\begin{aligned}\Delta T &\sim (1+z)\frac{r}{c}\Big[\cos(\max\{0, \vartheta_{\rm obs} - \Delta\theta_{\rm tot}\}) \\ &\quad - \cos(\vartheta_{\rm obs} + \Delta\theta_{\rm tot})\Big] \\ &\sim (1+z)\frac{r}{2c\gamma^2} \\ &\quad \times \begin{cases} (\gamma\vartheta_{\rm obs} + \gamma\Delta\theta_{\rm tot})^2, & \vartheta_{\rm obs} < \Delta\theta_{\rm tot} \\ 4(\gamma\vartheta_{\rm obs})(\gamma\Delta\theta_{\rm tot}), & \vartheta_{\rm obs} > \Delta\theta_{\rm tot} \end{cases} .\end{aligned}$$

In the following, we assume $z = 0$ for simplicity.

Let us consider the case of $\vartheta_{\rm obs} = 0$ (then, $n_s \sim 10^2$). Bright pulses in all the sub-jet emissions are observed when $\theta_v^{(j)} (= \vartheta^{(j)}) \lesssim \gamma^{-1}$. Then the observed duration of the brightest pulses can be calculated as $\delta T^{(j)} \sim 0.1\,{\rm sec}$, while $\Delta T \sim 70\,{\rm sec}$, therefore, $\delta T^{(j)} \ll T_{\rm dur} \lesssim \Delta T$. Brightest period lasts for about $T_{\rm dur}$. Since we assume $t_{\rm dep}^{(j)}$ (the departure time of each sub-jet at the central engine) is randomly distributed, brightest spikes in the observed light curve are uniformly distributed in this period. Since the mean time-interval between bright spikes is about $T_{\rm dur}/n_s \sim 0.3$ sec and is larger than the pulse duration $\delta T^{(j)}$, those are separated with each other. This period is followed by that with a duration of $\Delta T - T_{\rm dur} \sim 40$ sec in which low-flux soft events come from sub-jets with large $\theta_v^{(j)}$.

On the other hand, when all sub-jets are viewed off-axis, i.e., $n_s = 0$, observed time profile is greatly altered. In this case, $\delta T^{(j)}$ increases with the viewing angle and observed light curves become very smooth. Since we see the periphery emission, the number of observed (bright) pulses is small. For XRFs or X-ray rich GRBs with $\vartheta_{\rm obs} \sim \Delta\theta_{\rm tot}$ ($\vartheta_{\rm obs} \gg \Delta\theta_{\rm tot}$), the duration of bright emission period is comparable to or less than $\sim T_{\rm dur}$ (δT for smallest θ_v), while overall duration is given by ΔT. There may even be the case when the mean pulse interval in the observed light curve is smaller than the pulse duration and observed sub-jet emissions overlap with each other and merge like one or a few pulses. Therefore, variability of XRFs and X-ray rich GRBs is low. This is a possible explanation of observed E_p–variability relation [29]. More quantitative analysis is under investigation [56].

Fine Temporal Structures of Short GRBs. — It has been known that a large fraction of short bursts are composed of a few pulses with a duration of several tens of msec [33]. At present we use a very simple model of a subjet, i.e, instananeous emission at a certain radius. In reality there will be a distribution of Lorentz factor of subjet so that the faster one will collide to the slower ones. Observed variability of short bursts may arise in such a more comlicated modeling of subjet emissions.

Other Properties. — Some observers could see a cold spot with small n_s in the core to have a small geometrically corrected energy even if the total energy of the GRBs is the same. Thus our model may be compatible with the recent claim that the total kinetic energy has smaller dispersion than the geometrically corrected γ-ray energy [6, 7]. The X-ray pre-/post-cursor is also expected if off-axis sub-jets are ejected earlier (for precursor) or later (for postcursor) than the main sub-jets [31]. The viewing angle of the sub-jets may also cause the luminosity-lag/variability/width relations of the GRBs including GRB 980425 [19, 53].

4.3. Afterglow Properties

Early Afterglows. — At an early phase, the afterglow variabilities may arise from the angular energy fluctuations within the GRB jet [32, 34, 37], which might correspond to the inhmogeneous n_s. Indeed, in the context of the patchy shell model, the observed properties of variable afterglow of GRB 021004 are well explained if the angular size of the patches is about 0.02 rad [32]. This size is similar to those we adopt in this paper.

Late Phase Afterglows of XRFs. — The afterglow could have a different behavior between the core-

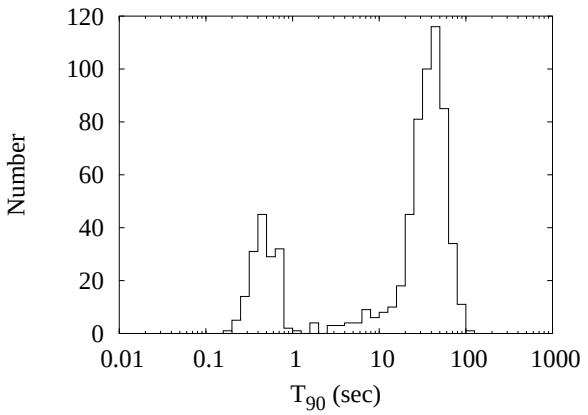

Figure 6: T_{90} duration distribution in 50–300 keV of hard events with observed fluence ratio $S(2-30\ \mathrm{keV})/S(30-400\ \mathrm{keV}) < 10^{-0.5}$. Subjet distribution is given by Gaussian form. The source redshifts are varied according to the cosmic star formation rate.

envelope sub-jet model and the uniform jet model. In the uniform jet model, the afterglows of XRFs should resemble the orphan afterglows that initially have a rising light curve [14, 51]. An orphan afterglow may be actually observed in XRF 030723 [10], but the light curve may peak too early [58]. The optical afterglow of XRF 020903 is not observed initially (< 0.9 days) but may not be consistent with the orphan afterglow [43]. These problems could be overcome by introducing a Gaussian tail with a high Lorentz factor around the uniform jet [58] because the energy redistribution effects may bring the rising light curve to earlier times [24, 58]. Therefore, as long as the observer points within or slightly off-axis to the whole jet (case B_1), the late phase ($\gtrsim 1$ day) properties of XRF afterglow may be similar to those of long GRBs. On the other hand, when the whole jet is viewed far from the edge of the jet, such that $\vartheta_{\rm obs} \gg \Delta\theta_{\rm tot}$ (case B_2), XRF afterglows may resemble the orphan afterglow (e.g., see the upper-left panel of fig. 5 in ref [24]. Afterglows for cases B_1 and B_2 may correspond $\theta_{obs} = 5.7^\circ$ and $\theta_{obs} = 11.5^\circ$ in ref [24], respectively). Because of the relativistic beaming effect, case B_2-like events are dimmer than case B_1-like events in both the prompt and afterglow phase (see Figure 4), so that they may be rarely observed, but we believe XRF 030723 is a member of such a class. Recent calculation for this subject can be found in [15].

Late Phase Afterglows of Short GRBs. — The afterglow of a short GRB may be difficult to predict since it could resemble both the orphan and normal afterglow depending on the sub-jet configuration within the envelope. One situation is considered in [8], where global afterglow emission is approximated by that of a Gaussian structured jet superimposed on a uniform jet. Then the emission is dominated by the on-axis sub-jet at relatively early times, while it is dominated by the more energetic Gaussian core at later times. This model assumes the void around the sub-jet that leads to an afterglow bump. On the other hand, if the sub-jet structure is produced by one whole jet through hydrodynamical instability (§ 4.1), the afterglow of short GRB may be similar to those of structured jet model because in this case the whole jet is entirely filled with kinetic energy (i.e., no void around the on-axis sub-jet).

4.4. Predictions of our Model

A clear prediction of our unified model is that short GRBs should be associated with energetic SNe[2]. Even if the SNe are not identified with short GRBs due to some observational reasons we predict that the spatial distribution of short GRBs in host galaxies should be similar to that of the long GRBs. Another prediction is that short GRBs should have the same total kinetic energies as long GRBs, which might be confirmed by radio calorimetry.

Interestingly our model has predicted short XRFs or short X-ray rich GRBs [55]. They are observed when isolated sub-jets are viewed slightly off-axis. The observed short XRF 040924 may be a kind of these bursts [9]. Note that the short XRFs will be longer than the short GRBs since the pulse duration grows as the viewing angle increases [19, 50]. The event rate of short XRFs will depend on the configuration of the sub-jets in the envelope. Further observations are necessary to determine the envelope structure.

4.5. Comment on the NS-NS Merger Model for short GRBs

Let us assume that short GRBs arises from coalescing binary neutron stars. Then the current estimate of the coalescing rate is about 10^{-4} y^{-1} galaxy^{-1} [21] while the event rate of long GRBs is estimated as $\sim 10^{-6}$ y^{-1} galaxy^{-1}. If we assume that the distance to short GRBs is similar to long GRBs, the isotropic energy of GRBs should be a hundredth of long GRBs because the luminosity of long and short GRBs are similar (Figure 1) and the duration of short burst is typically a hundredth of that of long GRB. From the event rate, the opening angle of the short GRB is an order of magnitude smaller than the long GRBs. The typical energy of long GRBs is about 10^{51} erg and the

[2]Indeed, one of short GRBs (GRB 970514) shows the possible association with a type IIn SN (SN 1997cy) [11], however, it may be probable that it was one of rare SN Ia events exploding in a dense circumstellar medium [46].

typical opening half-angle is ~ 0.1. This suggests that the total energy of short GRBs is about 10^{47} erg, while $\sim 10^{52}$ erg is liberated from the coalescence of binary neutron star. This means that the short burst is much less effective and much less energetic compared to long GRB.

Acknowledgments

R.Y. thanks the conference organizers for inviting him to present this paper and for partial support. This work was supported in part by a Grant-in-Aid for Scientific Research of the Japanese Ministry of Education, Culture, Sports, Science and Technology, No.05008 (RY), No.14047212 (TN), and No.14204024 (TN) and also in part by the Eberly Research Funds of Penn State and by the Center for Gravitational Wave Physics under grants PHY-01-14375 (KI).

References

[1] Aloy, M. A., Ibáñez, J.-M., Miralles, J.-A., & Urpin, V. 2002, A&A, 396, 693
[2] Amati, L., et al. 2002, A&A, 390, 81
[3] Antonucci, R. 1993, ARA&A, 31, 473
[4] Awaki, H., Koyama, K., Inoue, H., & Halpern, J. P. 1991, PASJ, 43, 195
[5] Balázs, L. G., Bagoly, Z., Horváth, I., Mészáros, A., & Mészáros, P. 2003, A&A, 401, 129
[6] Berger, E., et al. 2003, Nature, 426, 154
[7] Bloom, J. S, Frail, D. A., & Kulkarni, S. R. 2003, ApJ, 594, 674
[8] Fan, Y. Z. et al. 2004, astro-ph/0410060
[9] Fenimore, E. Ricker, G., Atteia, J-L, et al., 2004, GCN Circ. 2735
[10] Fynbo, J. P. U., Sollerman, J., Hjorth, J. et al., 2004, ApJ. 609, 962
[11] Germany, L. M., Reiss, D. J., Sadler, E. M. et al., 2000, ApJ, 533, 320
[12] Ghirlanda, G., Ghisellini, G., & Celotti, A., 2004, A&A, 422, L55
[13] Gomez, E. A. & Hardee, P. E. 2003, astro-ph/0311134
[14] Granot, J., Panaitescu, A., Kumar, P., & Woosley, S. E., 2002, ApJ, 570, L61
[15] Granot, J., Ramirez-Ruiz, E., & Perna, R., 2005, astro-ph/0502300
[16] Heise, J., in 't Zand, J., Kippen, R. M., & Woods, P. M., 2001, in Proc. Second Rome Workshop: Gamma-Ray Bursts in the Afterglow Era, ed. E. Costa, F. Frontera, & J. Hjorth (Berlin: Springer), 16
[17] Hjorth, J., Sollerman, J., Möller, P. et al., 2003, Nature, 423, 847
[18] Huang, Y. F., Wu, X. F., Dai, Z. G., Ma, H. T., & Lu, T. 2004, ApJ, 605, 300
[19] Ioka, K., & Nakamura, T., 2001, ApJ, 554, L163
[20] Ioka, K., & Nakamura, T. 2002, ApJ, 570, L21
[21] Kalogera, V. et al. 2004, ApJ, 601, L179
[22] Kippen, R. M., Woods, P. M., Heise, J. et al. 2002, AIP Conf. Proc. 662, 244 (astro-ph/0203114)
[23] Kouveliotou, C., et al. 1993, ApJ, 413, L101
[24] Kumar, P., & Granot, J., 2003, ApJ, 591, 1075
[25] Kumar, P., & Piran, T. 2000, ApJ, 535, 152
[26] Lamb, D. Q. 2002, astro-ph/0206151
[27] Lamb, D. Q. et al. 2004, New Astron. Rev. 48, 423 (astro-ph/0309462)
[28] Lloyd-Ronning, N. M., Dai, X., & Zhang, B. 2004, ApJ, 601, 371
[29] Lloyd-Ronning, N. M. & Ramirez-Ruiz, E. 2002, ApJ, 576, 101
[30] Mészáros, P. 2002, ARA&A, 40, 137
[31] Nakamura, T., 2000, ApJ, 534, L159
[32] Nakar, E. & Oren, Y. 2004, ApJ, 602, L97
[33] Nakar, E. & Piran, T. 2002, MNRAS, 330, 920
[34] Nakar, E., & Piran, T. 2003, ApJ, 598, 400
[35] Paciesas, W. S. et al. 1999, ApJS, 122, 465
[36] Piran, T. 1999, Phys. Rep. 314, 575
[37] Piran, T., Nakar, E., & Granot, J. 2003, astro-ph/0312138
[38] Ramirez-Ruiz, E., Celotti, A., & Rees, M. J. 2002, MNRAS, 337, 1349
[39] Ramirez-Ruiz, E. & Fenimore, E. E. 2000, ApJ, 539, 712
[40] Rossi, E., Lazzati, D., & Rees, M. J. 2002, MNRAS, 332, 945
[41] Sago, N., Ioka, K., Nakamura, T., & Yamazaki, R., 2004, Phys. Rev. D 70, 104012
[42] Sakamoto, T., Lamb, D. Q., Graziani, C. et al., 2004, ApJ, 602, 875
[43] Soderberg, A. M., Kulkarni, S. R., Berger, E. et al., 2004, ApJ, 606, 994
[44] Stanek, K. Z. Matheson, T., Garnavich, P. M. et al., 2003, ApJ, 591, L17
[45] Toma, K., Yamazaki, R., & Nakamura, T., 2005, ApJ, 620, 835
[46] Turatto, M. et al., 2000, ApJ, 534, L57
[47] Urry, C. M. & Padovani, P. 1995, PASP, 107, 803
[48] Watson, D., et al. 2004, ApJ, 605, L101
[49] Yamazaki, R. 2004, Ph.D. THESIS, Kyoto University
[50] Yamazaki, R., Ioka, K., & Nakamura, T., 2002, ApJ, 571, L31
[51] Yamazaki, R., Ioka, K., & Nakamura, T., 2003a, ApJ, 591, 283
[52] Yamazaki, R., Ioka, K., & Nakamura, T., 2003b, ApJ, 593, 941
[53] Yamazaki, R., Yonetoku, D., & Nakamura, T., 2003c, ApJ, 594, L79
[54] Yamazaki, R., Ioka, K., & Nakamura, T., 2004a, ApJ, 606, L33

[55] Yamazaki, R., Ioka, K., & Nakamura, T., 2004b, ApJ, 607, L103
[56] Yamazaki, R. et al. 2005, in preparation
[57] Yonetoku, D., et al. 2004, ApJ, 609, 935
[58] Zhang, B., Dai, X., Lloyd-Ronning, N. M., & Mészáros, P., 2004, ApJ, 601, L119
[59] Zhang, B., & Mészáros, P. 2002, ApJ, 571, 876
[60] Zhang, B., & Mészáros, P. 2004, Int. J. Mod. Phys. A19, 2385 (astro-ph/0311321)
[61] Zhang, W., Woosley, S. E., & Heger, A. 2004, ApJ, 608, 365